

High-spin states in the odd-odd nucleus ^{92}Tc

S. S. Ghugre and S. B. Patel

Department of Physics, University of Bombay, Vidyanagari, Bombay 40 0098, India

R. K. Bhowmik

Nuclear Science Centre, Aruna Asaf Ali Marg, New Delhi 11 0067, India

(Received 24 November 1993; revised manuscript received 1 September 1994)

This work presents for the first time the high-spin information on the odd-odd neutron deficient nucleus ^{92}Tc . We have used the reaction $^{64}\text{Zn}(^{35}\text{Cl}, 4p3n)^{92}\text{Tc}$ at a beam energy of 140 MeV to populate high-spin states in the $N = 49$ nucleus ^{92}Tc . Gamma-ray intensities and $\gamma-\gamma$ coincidences were measured. Nineteen new transitions have been found and placed in a level scheme. The positive and negative parity bands have been extended tentatively up to a spin of 17^+ and 21^- , respectively. The level scheme can be reasonably well understood within the $(p_{1/2}, g_{9/2})$ model space and breaking of the $N = 50$ neutron core. We have observed two discrepancies in the earlier work on the low-lying states in ^{92}Tc .

PACS number(s): 23.20.Lv, 23.20.En, 21.60.Cs, 27.60.+j

I. INTRODUCTION

The present work is a part of our attempt to systematically study the high-spin states of nuclei at and near the neutron magic number $N = 50$. It gives the first high-spin data on the odd-odd neutron-deficient nucleus ^{92}Tc . We had earlier reported our study of high-spin states in ^{93}Tc [1] and ^{95}Ru [2].

The low-lying states in these nuclei are well described by taking ^{88}Sr as the core and the valence nucleons occupying the $(p_{1/2}, g_{9/2})$ configuration space [3,4]. However, to describe the observed high-spin states in these nuclei, lying at or near the neutron magic number $N = 50$, an enlarged configuration space is needed [1]. Another possible mechanism to generate the higher angular momentum states is to break the $N = 50$ neutron core [5]. Therefore, it appeared interesting to systematically explore the high-spin states in the $N = 50$ and neighboring nuclei, in order to understand the possible mechanism for generating these states.

The ^{92}Tc nucleus with 43 protons and 49 neutrons is characterized by the simplifying feature that only one high-spin orbital $g_{9/2}$ is available. This makes the shell model as a good starting point for the description of ^{92}Tc . To understand the structure at the highest spins, we have attempted the breaking of the $N = 50$ neutron shell. The observed level scheme of ^{92}Tc is found to be reasonably well described by this approach.

II. EXPERIMENTAL DETAILS AND ANALYSIS

The isotopically enriched ($\sim 99\%$) ^{64}Zn target had a thickness of about 1.3 mg cm^{-2} on a 25 mg cm^{-2} Pb backing. The heavy-ion beam of ^{35}Cl was delivered by the 15 UD Pelletron accelerator at the Nuclear Science Centre (NSC) at New Delhi. The energy of the beam chosen was 140 MeV. This energy was chosen because our

main interest was to investigate the high-spin behavior of ^{95}Rh and $^{94,95}\text{Ru}$ nuclei, and so their yields were kept maximum compared to other nuclei like ^{93}Tc and ^{92}Mo , which were also produced in the same reaction. The relative production cross section of the residues in this heavy ion reaction (^{35}Cl on ^{64}Zn at $E_{\text{lab}} = 140 \text{ MeV}$) were consistent with those predicted by the statistical model code CASCADE using the parameters reported by Dasgupta *et al.* [6].

When the data were analyzed, we found that even though we had not optimized the incident beam energy for the $(4p3n)$ channel which leads to ^{92}Tc , we had interesting new information about the ^{92}Tc nucleus at high spin, with reasonable statistics.

$\gamma-\gamma$ coincidences were measured using the gamma detector array (GDA), at the NSC. At the time of this experiment the GDA consisted of five Compton-suppressed high-purity germanium detectors and a 14-element bismuth germanate (BGO) multiplicity filter. The details of the GDA can be found in Ref. [1], wherein we had reported the high-spin spectroscopy of ^{93}Tc . The typical energy resolution of the germanium detectors was about 2 keV at 1 MeV.

Previous study of ^{92}Tc by Fields *et al.* [7] had used the light projectile, ^3He , at a beam energy of 33 MeV, on a ^{92}Mo target. In the present work, a heavy ion beam of ^{35}Cl has been employed at a beam energy of 140 MeV. This significantly changed the situation—the higher angular momentum states in ^{92}Tc were excited. As a result we observed the yrast states in ^{92}Tc and the low-lying nonyrast levels reported by Fields *et al.* [7] were not observed by us.

The ^{92}Tc γ rays have been placed in the level scheme using the observed coincidence relationship and intensity argument for the γ rays. The typical γ coincidence rate was about 150 counts per second and the events corresponding to a twofold or higher-fold coincidence (within a system timing resolution of 40 ns) were recorded in the

list mode. The list mode data consisted of a pattern word identifying the detectors in coincidence, their energies, the multiplicity information, and the timing information between two coincident γ rays. The timing information was recorded using the time-to-digital converters (TDC) [8]. The singles were gated with $K > 2$ condition, where K was the number of BGO elements that had fired in the multiplicity filter. In all about 30 million multiparameter events were collected.

The pulse height in all the detectors were software gain matched and the data was sorted into a $1024 \times 1024 E_\gamma - E_\gamma$ matrix (after appropriate software gain matching to 1 keV per channel). In all six such $1024 \times 1024 E_\gamma - E_\gamma$ matrices were formed, to cover the energy range up to 3 MeV. From the processed data, background-subtracted one-dimensional histograms for γ energies in one detector gated by a suitable transition in the other detector could be generated. The FWHM of a clean peak at about 1 MeV, used in the analysis was about two channels (the calibration being 1 keV per channel). The amplifier gains in the experiment were kept low enough so that γ rays up to 2.7 MeV could be recorded. Figure 1 shows the total projection spectrum; the strong transitions in the different exit channels are marked. The present configuration of the gamma detector array allows us to put detectors at 99° and at 153° with respect to the beam direction. Multipolarities of the transitions were extracted assuming stretched transitions using the DCO (directional correlations from oriented nuclei) procedure described in details in Refs. [1,9]. We outline the procedure followed by us briefly: In order to assign multipolarities to the observed transitions, the data were sorted out into an $E_\gamma - E_\gamma$ matrix, such that the events recorded in the detectors at 99° with respect to the beam direction were plotted along the y axis (after appropriate software gain matching to 1 keV per channel). The data from the other group of detectors, at 153° with respect to the beam direction were then plotted along the x axis. Following the procedure described in Refs. [1,9], a gate corresponding to a γ ray of known multipolarity, is taken for the detec-

tors on the x axis and the γ ray spectrum for detectors along y axis is projected through it. Next, the same gate is taken for the y axis detectors and the γ spectrum for detectors along the x axis is projected through it. Assuming stretched transitions, the intensities of those γ rays which have the same multipolarity as the gated γ ray will be equal in both the projected spectra. On the other hand, the intensities differ by a factor of about 2 in the two projections, if the multiplicities of the projected γ rays are different. The drawback of this method is that it is difficult to estimate any possible $M1, E2$ admixtures which cannot be ruled out. For this reason all the multiplicities deduced by us are only tentative and so we have put them in a bracket in Fig. 5.

III. EXPERIMENTAL RESULTS

In this experiment we have observed nineteen new γ rays, belonging to the nucleus ^{92}Tc . The relative intensities were extracted from the singles data. Some of the γ rays in ^{92}Tc were identical in energy with the γ rays emitted by neighboring nuclei which were also produced. For example, the 484 keV transition was present in both ^{92}Tc and ^{93}Tc nuclei. We have used gated spectra for the intensity determination of these ‘‘contaminated’’ γ ray peaks in the singles spectrum. Table I gives the excitation energy (E_x), transition energy (E_γ), the relative intensity (I_γ), and the spin assignment of the γ rays. All the intensities were efficiency corrected.

Our angular correlation data indicated that the in-band 646 keV transition corresponds to a stretched quadrupole (i.e., it involves a change in angular momentum by two units), so we have tentatively assigned an $E2$ character to the 646 keV γ ray. This fact coupled with the coincidence data showed that the 545 keV γ ray connected the 12^+ state to the 12^- state. Figure 2 shows the projected spectrum with 545 keV transition as the gate. This transition belongs to the negative parity band. The new γ rays observed in this band were 70(M1),

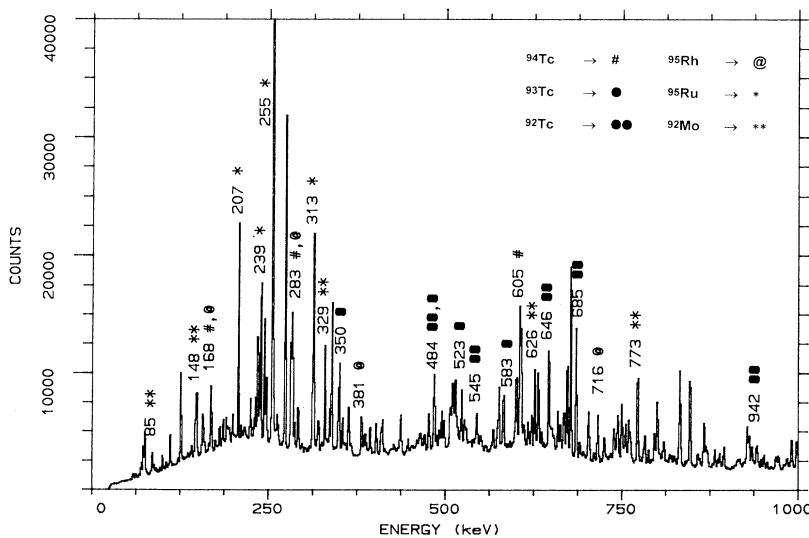


FIG. 1. Total projection spectrum up to 1 MeV. The strong transitions in the different channels are marked. All transition energies are marked within ± 1 keV.

TABLE I. Excitation energy (E_x), transition energy (E_γ), relative intensity (I_γ), and spin assignment of the γ rays belonging to ^{92}Tc .

E_x (keV)	E_γ (keV)	I_γ	$J_i \rightarrow J_f$
1354.7	1354.7	100.0 (5)	$10^+ \rightarrow 8^+$
685.7	685.7	16.7 (2.0)	$9^+ \rightarrow 8^+$
1354.7	668.9	^a	$10^+ \rightarrow 9^+$
4590.1			$16^{(-)} \rightarrow 15^{(-)}$
2001.0	646.4	85.0 (5)	$(12^+) \rightarrow 10^+$
2663.9	662.8	22.6 (1.2)	$(13^+) \rightarrow (12)$
3299.9	636.1	9.4 (8)	$(14^+) \rightarrow (13^+)$
3586.7	286.7	9.5 (6)	$(15^+) \rightarrow (14^+)$
5645.1	2058.5	10.0 (4.0)	$(17^+) \rightarrow (15^+)$
6271.9	626.7	$< 2^c$	
3066.8	1066.1	27.7 (1.1)	$13^{(-)} \rightarrow (12^+)$
2545.8	544.8	39.3 (5)	$12^{(-)} \rightarrow (12^+)$
3066.8	520.9	7.7 (1.4)	$13^{(-)} \rightarrow (12^+)$
3561.4	1015.2	1.6 (2.8)	$14^{(-)} \rightarrow 12^{(-)}$
3561.4	494.6	16.4 (1.3)	$14^{(-)} \rightarrow 13^{(-)}$
4045.8	484.1	$< 20.0^c$	$15^{(-)} \rightarrow 14^{(-)}$
4784.2	738.4	$< 10.0^c$	$17^{(-)} \rightarrow 15^{(-)}$
4784.2	69.9	$< 1.0^c$	$17^{(-)} \rightarrow 16^{(-)}$
6722.6	1938.4	2.8 (6.3)	$19^{(-)} \rightarrow 17^{(-)}$
7830.5	1107.9	9.7 (8)	$21^{(-)} \rightarrow 19^{(-)}$
2939.2	393.4	17.6 (1.2)	$(12^+) \rightarrow 12^{(-)}$
3561.4	621.9	$< 8.0^c$	$14^{(-)} \rightarrow (12^+)$
3066.8	127.6	^b	$13^{(-)} \rightarrow (12^+)$
4613.0	1051.6	3.0 (1.3)	
6031.8	1985.9	4.0 (5.0)	

^a I_γ could not be computed as the 669 keV transition is a doublet.

^b I_γ could not be computed from singles due to contribution from some unknown contaminant.

^cIndicates that the I_γ has been computed from the coincidence spectra.

128,484(M1), 495(M1), 521(M1), 622(M2), and 669(M1), 738(E2), 1015(E2), 1108(E2), 1938(E2), 1066(E1), 1052, and 1986 keV. The 1066 keV transition corresponds to a stretched dipole (i.e., it involves a change in the angular momentum by 1 unit). Since this γ ray connects the positive and negative parity bands we have tentatively put its character as E1. The level at an excitation energy of 2939 keV poses some problem in the assignment of the spin and parity. The multiplicities of the transitions were extracted assuming stretched transitions. As stated before, the possible presence of admixtures makes these predictions somewhat tentative. Accordingly, our data tentatively enables us to conclude that the 393 keV transition corresponds to a stretched dipole (i.e., it involves a change in the angular momentum by 1 unit). If the 2939 keV level had a spin parity of 13^+ , then we would have surely found a 939 keV γ ray, which would have resulted from the preferable decay of the 2939 keV level to the (12^+) level in the positive parity band. The absence of this 939 keV γ ray makes the 13^+ assignment for the 2939 keV level less likely. We feel that the 2939 keV level could well be the second 12^+ level and have put this tentative assignment in bracket. The shell model results are also consistent with this conclusion. These calcula-

tions are described in the next section. In view of this, we have assigned M2 character to the 622 keV transition. However, we could not assign any multipolarity to the 128 keV transition. The two γ rays 1986 and 1052 keV were very weak and so no tentative conclusion about their multipolarity could be drawn.

Figure 3 shows the projected spectrum with 636 keV transition as the gate. This transition belongs to the positive parity band. The new γ rays observed in this band were 287(M1), 636(M1), 627, and 2059 (E2) keV. As seen in the spectrum gated by the 636 keV γ ray, the 646 keV ($12^+ \rightarrow 10^+$) transition is stronger than the 663 keV ($13^+ \rightarrow 12^+$) transition. This may be due to either a two transition connection between the (13^+) and the (12^+) levels parallel to the 663 keV transition, or that the 646 keV transition is a doublet. Based on the data our conclusion is that the 646 keV transition is not a doublet. The other possibility of a two-transition connection between the (13^+) and the (12^+) levels, parallel to the 663 keV transition, may be plausible. There is a weak 640 keV transition in the 636 keV gated spectrum. However, the difference (663–640 keV) being 23 keV, we could not pursue this possibility, since we were not in a position to detect low-energy γ rays up to about 40 keV.

The 669 keV transition was in coincidence with itself (Fig. 4) implying that there are two γ rays of the same energy 669 keV. As seen from Fig. 4, the 663 keV transition is weak in this gated spectrum. Its intensity should at least be half that of the 545 keV transition, a fact that we have observed in the 1355, 686, and 646 keV gates. The fact that the 669 keV transition is a doublet with one member in the positive parity band ($10^+ \rightarrow 9^+$) and the other in the negative parity band ($16^{(-)} \rightarrow 15^{(-)}$), we feel can explain the observed weak intensity of the 663 keV transition in the 669 keV gate. The 545 keV ($12^{(-)} \rightarrow (12^+)$) transition is in coincidence with both the 669 keV γ rays ($16^{(-)} \rightarrow 15^{(-)}$) and ($10^+ \rightarrow 9^+$), unlike the 663 keV ($13^+ \rightarrow 12^+$) transition which sees only one 669 keV ($10^+ \rightarrow 9^+$) γ ray.

We have observed that the 669 keV ($10^+ \rightarrow 9^+$) transition was stronger than the 686 keV ($9^+ \rightarrow 8^+$) transition. This indicated that there could be several decays from the 9^+ level. These could be by the emission of small energy γ rays which we did not observe in this experiment. In addition to the new transitions mentioned above a 194 keV M1 γ ray was observed belonging to ^{92}Tc . We have not been able to place this transition in the decay scheme.

We have gated on all the γ rays and looked at the intensity flow above and below the gated γ ray and feel reasonably certain about the position of these γ rays in the level scheme. The proposed level scheme for ^{92}Tc is shown in Fig. 5. Newly observed γ rays in the present work have been indicated with dots. Several cross transitions were found in the negative parity band. These were 738(E2), 1015(E2), 1066(E1), and 1938(E2) keV. For example, the gated spectrum for the in-band 1015 keV cross transition shows that the two γ rays 521 and 495 keV were absent, while all other members of the negative parity band were present. Similarly, a gate on either the 521 or 495 keV γ rays showed that the 1015 keV γ ray was not in coin-

cidence with them, while all other members of the band were. The existence of this and other cross transitions makes the proposed level scheme very likely; the depopulation pattern gets tied down. The spins and parities indicated in Fig. 5 are somewhat tentative, since due to possibility of the presence of short lived ($\sim 0.1 - 1$ ns) isomers in this near closed shell nucleus (^{92}Tc), the angular correlations may be attenuated and many γ rays may be unstretched. Admixtures also cannot be ruled out. We have therefore indicated the spin parities in brackets in Fig 5. The positive parity band has been extended up to a tentative spin of $J = 17^+$, corresponding to an excitation energy of 6.2 MeV. The negative parity band has been extended up to a tentative spin of $J = 21^-$ and an excitation energy of 7.8 MeV.

We have found discrepancies in the earlier work on low-lying levels in ^{92}Tc . In an earlier work by Fields *et al.* [7], a 147 keV γ ray in cascade with 545-647-1355 keV transition was reported. However, in the 545 keV gate (Fig. 2) there is a strong 147 keV transition. Our coin-

cidence data unambiguously indicated that this 147 keV transition does not belong to ^{92}Tc . This transition was not in coincidence with the 646 keV transition. Figure 6 depicts this situation. The 147 and 1392 keV transitions which appear in the 545 keV gate belong to ^{93}Ru . A major discrepancy was found in another earlier work by Ishii *et al.* [10] who had reported that there is a new γ ray sequence, 257-500-1347 keV in ^{92}Tc . Our coincidence data unambiguously indicates that the 1347 keV transition is feeding the 71 μs isomeric level in ^{94}Ru at an excitation energy of 2.6 MeV. A study using the same reaction used to populate ^{92}Tc is currently in progress. Furthermore, the 500 and 257 keV γ rays also belong to ^{94}Ru , and so none of these three γ rays originate from ^{92}Tc .

IV. THEORETICAL DISCUSSIONS

The low-lying levels of $N=49$ isotones ^{88}Y , ^{89}Zr , ^{90}Nb , ^{91}Mo , and ^{92}Tc are well studied within

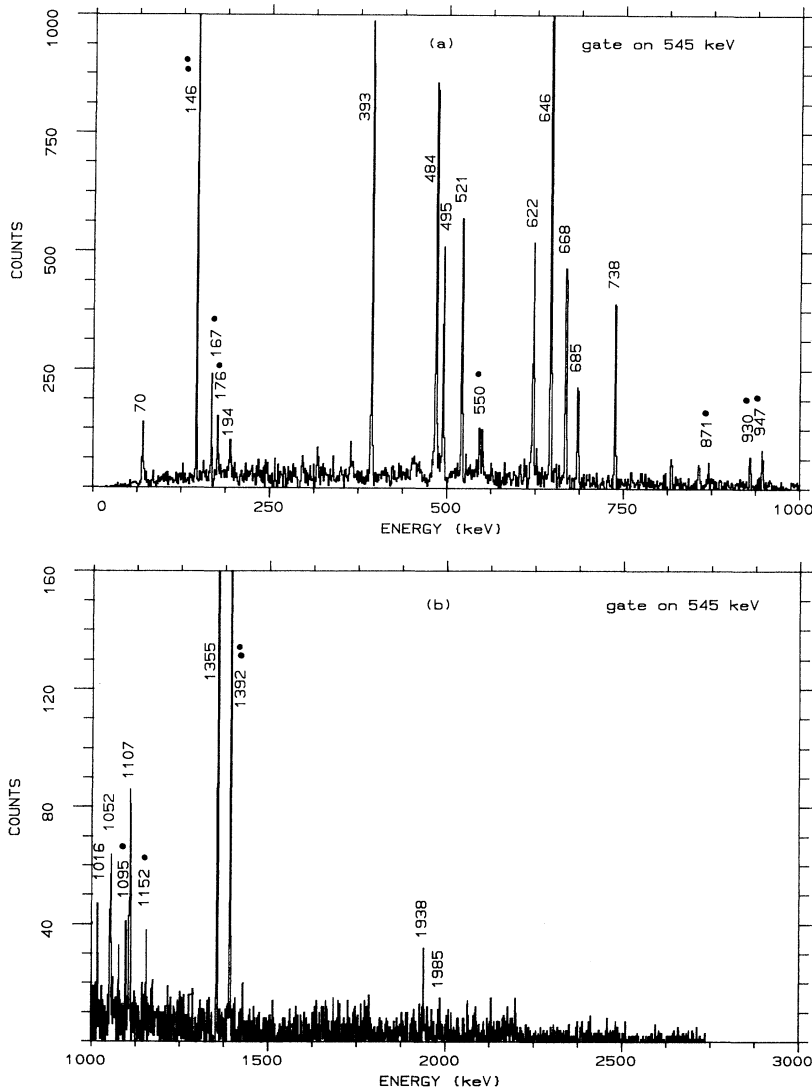


FIG. 2. γ - γ coincidence spectrum for ^{92}Tc with gate on the gamma transition 545 ($12^- \rightarrow 12^+$) keV transition. All transition energies are marked within ± 1 keV. The transitions marked with two dots belong to ^{93}Ru , while those marked with a single dot belong to some unknown contaminant.

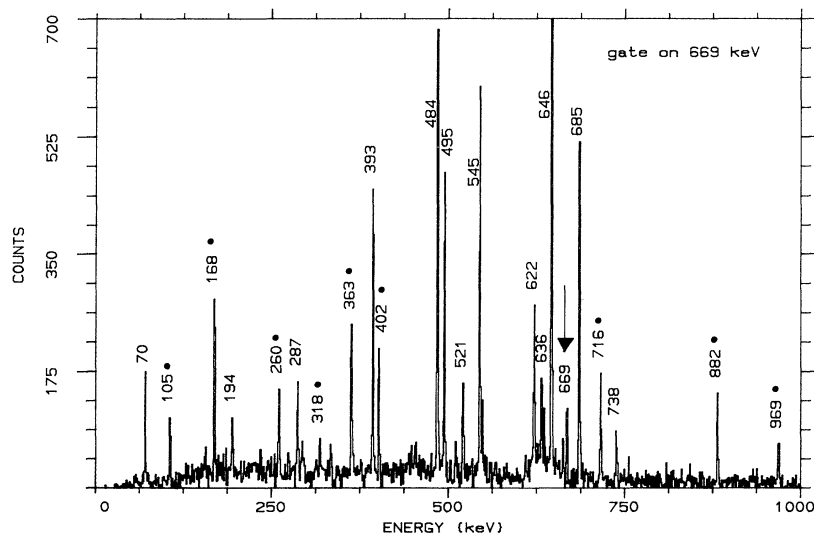
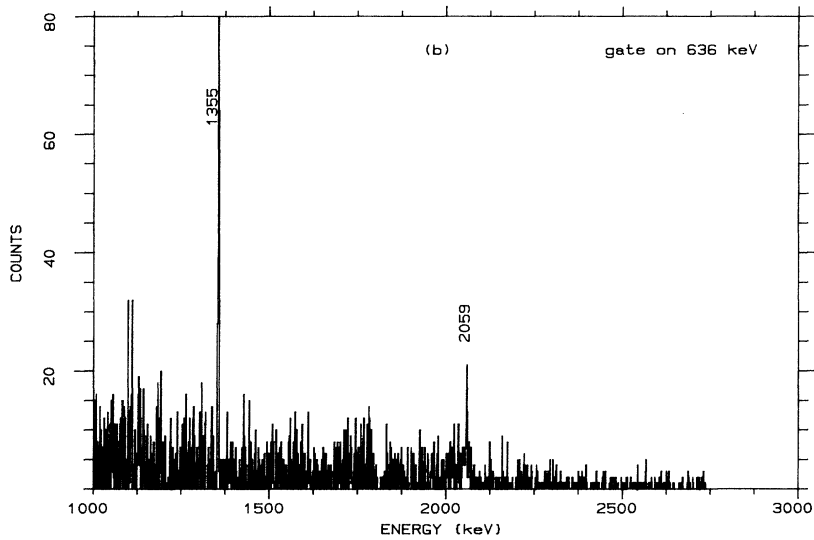
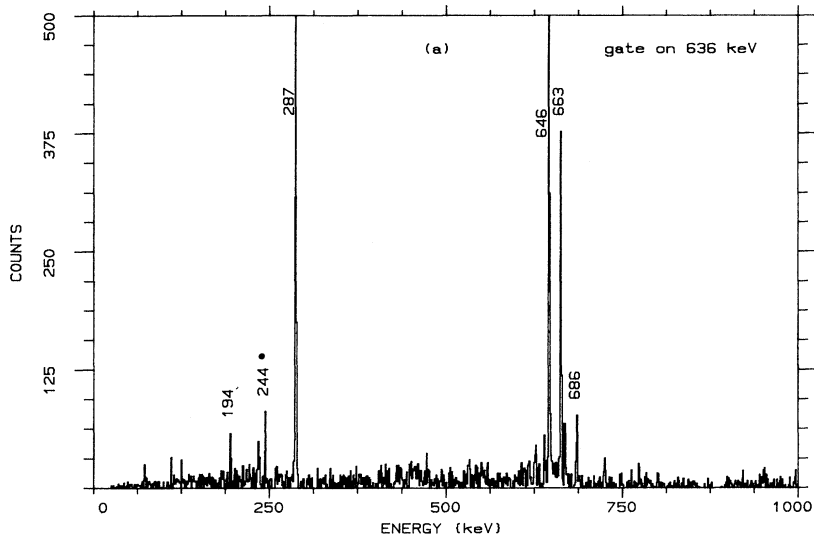


FIG. 3. γ - γ coincidence spectrum for ^{92}Tc with gate on the gamma transition 636 ($14^+ \rightarrow 13^+$) keV transition. All transition energies are marked within ± 1 keV. The transition marked with a dot belongs to some unidentified contaminant.

FIG. 4. Partial γ - γ coincidence spectrum with gate on 669 keV transition. The presence of another 669 keV γ ray indicates that the 669 keV γ ray is in coincidence with itself. The transitions marked with a dot belong to some unknown contaminant. All transition energies are marked within ± 1 keV.

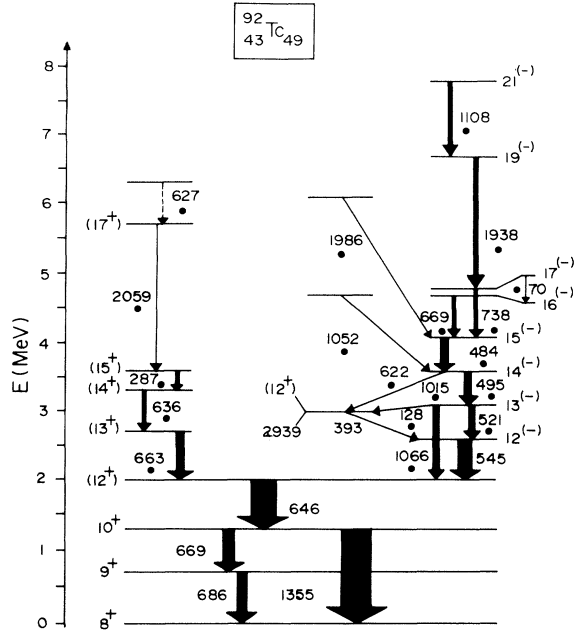


FIG. 5. Level scheme for ^{92}Tc showing the excitation and gamma transition energies for levels populated in $^{64}\text{Zn}(^{35}\text{Cl}, 4p3n)^{92}\text{Tc}$ reaction. The width of the arrows is approximately equal to the intensity of the transitions except the arrows indicating the 393, 622, 1052, and 1986 keV transitions.

the framework of the shell model with valence nucleons occupying the $p_{1/2}, g_{9/2}$ single-particle levels [11]. Gross and Frenkel [12] have computed the low-lying energy spectra for the $N = 49$ isotones by considering ^{88}Sr as a core and a model space consisting of the $\pi(p_{1/2}, g_{9/2})$ orbitals and the $\nu(p_{1/2}, g_{9/2})$ hole orbitals. The effective interaction for this model space was derived using 95 experimental energy levels of $N = 50$ and 49 isotones. Figure 7 shows the comparison of the experimental and calculated

energy levels [12], for ^{92}Tc , up to a spin of $J = 17$, the maximum angular momentum possible within this model space.

Serduke *et al.* [11] have deduced three sets of matrix elements for the proton particle neutron hole effective interaction in the $p_{1/2}-g_{9/2}$ model space. The 20 matrix elements of the effective interaction which define completely the shell model configuration space of active $p_{1/2}, g_{9/2}$ protons and neutrons were fit to 63 energy levels in the $N = 49$ nuclei. The three sets in Ref. [11] are (a) in which all matrix elements of the effective interaction were treated as free parameters, (b) in which the effective interaction was required to conserve the $T = 1$ seniority, and (c) in which only the $T = 0$ matrix elements of the effective interaction were adjusted. Out of these three sets of matrix elements we have done shell model calculations for ^{92}Tc for two sets within the model space consisting of the $(p_{1/2}, g_{9/2})$ active orbitals outside the ^{76}Sr as the core. The two sets were (b) and (c) (code named SLGM and SLGMO in OXBASH [13]) as mentioned above. The shell model code OXBASH was used for the calculations. For set (b) the effective interaction used was “seniority fit total energy” pp and nn interaction from Serduke and Gloeckner (SG) interaction [4], and for set (c) “ $T = 0$ ” pp and nn interaction from SLG interaction [14]. However the maximum angular momentum possible with 5 protons and 11 neutrons in the $(p_{1/2}, g_{9/2})$ orbitals outside the ^{76}Sr core is $J = 17$. Figure 8 shows a comparison of the experimental and calculated excitation energies. As seen from the figure there exists a fair agreement between the experimental and theoretical level structures. The presence of one $g_{9/2}$ orbital simplifies the shell model calculations for $N = 49$ isotones to a great deal, by describing most of the observed high-spin states (up to $20\hbar$) in these nuclei.

There exist two possible mechanisms to generate the high angular momentum states. The first and the obvious way is to employ a larger configuration space. Recently shell model calculations [15] have been performed for ^{92}Tc using ^{100}Sn as the core and the active

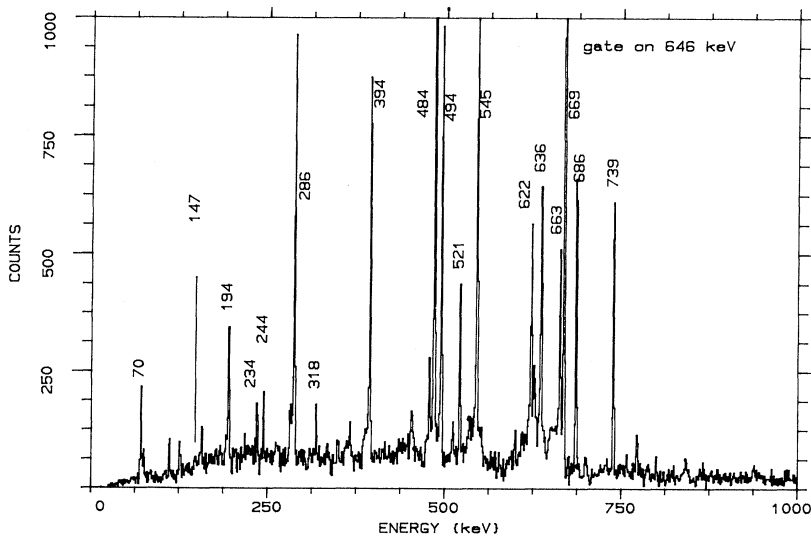


FIG. 6. γ - γ coincidence spectrum for ^{92}Tc with gate on the gamma transition 646 ($12^+ \rightarrow 10^+$) keV transition. The 147 keV transition reported by Fields *et al.* [7] is absent. This transition belongs to ^{93}Ru . All transition energies are marked within ± 1 keV.

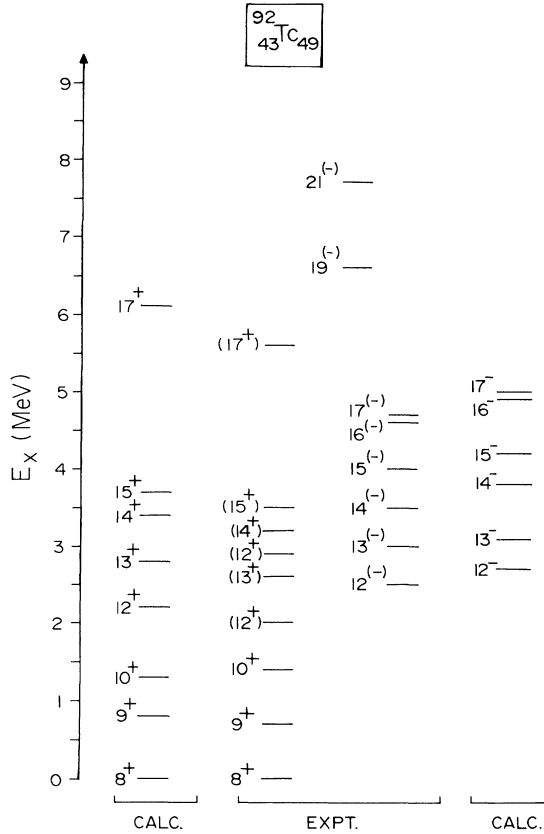


FIG. 7. Comparison of the experimental and calculated energy levels of ^{92}Tc as calculated by Gross *et al.* [12].

($0g_{9/2}, 1p_{1/2}, 1p_{3/2}, 0f_{5/2}$) proton hole orbitals. However, these calculations were not extended to high-spin regimes due to nonavailability of any experimental data. The problem with such a large basis space is that the energy matrices have very large dimensions, and unrestricted calculations become prohibitive due to memory limitations. The excitation of a neutron from the $0g_{9/2}$ orbit into the $1d_{5/2}$ orbit across the $N = 50$ core, appears to be a plausible mechanism for generating the observed higher angular momentum states. It is expected that the observed higher angular momentum states in these nuclei would be adequately described within a model space which allows for the excitation of the neutron across the $N = 50$ core, and also encompasses a large proton model space. However, due to computational difficulties a truncation scheme had to be developed to make these calculations feasible. The details of the truncation scheme are described in Ref. [16].

Calculations were performed within a model space (code named *GWB*, in *OXBASH* [13]), consisting of ^{66}Ni as the closed core and the $\pi\{0f_{5/2}, 1p_{3/2}, 1p_{1/2}, 0g_{9/2}\} : \nu\{1p_{1/2}, 0g_{9/2}, 0g_{7/2}, 1d_{5/2}, 1d_{3/2}, 2s_{1/2}\}$ orbitals. The effective interaction used was code named *GWBXC* in *OXBASH* [13]. The 974 two-body matrix elements (TBME) were generated from the bare matrix of Hosaka *et al.* Within this model space the 65 TBME for the $\pi(0f_{5/2}, 1p_{3/2}, 1p_{1/2}, 0g_{9/2})$ were taken from the Ji and

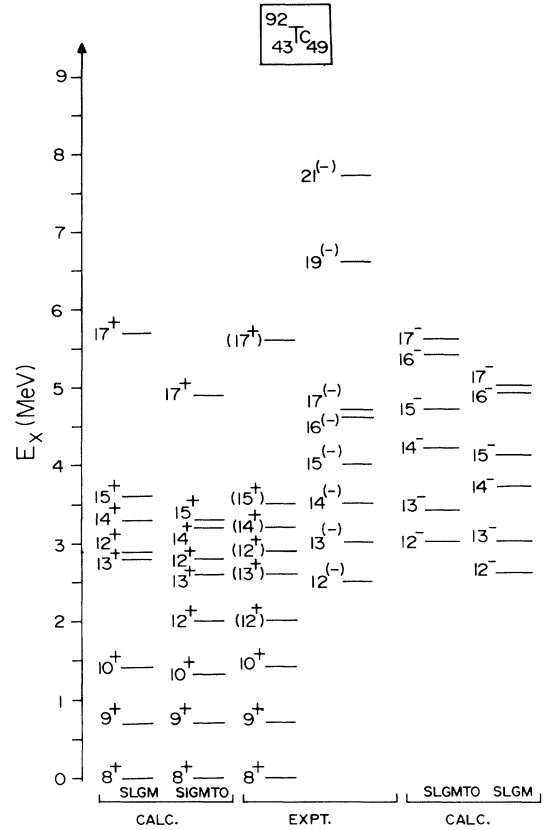


FIG. 8. Comparison of the observed states in ^{92}Tc with spherical shell model calculations within the ($p_{1/2}, 0g_{9/2}$) model space.

Wildenthal interaction. The 36 TBME connecting the $\pi(1p_{1/2}, 0g_{9/2})$ and $\nu(1d_{5/2}, 2s_{1/2})$ were taken from Lawson and Gloeckner interaction. The TBME for the $\pi(1p_{1/2}, 0g_{9/2})$ and $\nu(1p_{1/2}, 0g_{9/2})$ were taken from the Serduke, Lawson, and Gloeckner interaction. The TBME connecting the $\pi(1p_{1/2}, 0g_{9/2})$ and $\pi(1p_{1/2}, 0g_{9/2})$ were taken from Ball and McGrory's modified surface delta interaction. Figure 9 shows a comparison between the experimental and calculated energy spectra. As seen from the figure there exists a good agreement between the two up to a spin of $J = 17$. The excitation of a neutron across the $N = 50$ closed core requires an excitation energy of around 7 MeV in the unperturbed picture. This gap is reduced to about 2 MeV in this mass region due to many-body correlations. Hence it seemed interesting to perform these calculations within a still larger model space, where it was expected that the two-body matrix elements would take into account the effect of the many particle correlations in a more appropriate manner.

Accordingly, calculations were performed within a larger model space and corresponding effective interaction (code named *GLEPN* in *OXBASH* [13]). This model space consists of ^{56}Ni as the core and the $\{0f_{5/2}, 1p_{3/2}, 1p_{1/2}, 0g_{9/2}, 1d_{5/2}, 1d_{3/2}, 2s_{1/2}\}$ proton and neutron orbitals. As seen from Fig. 9, there is much better agreement for the levels above $J = 17^-$. This in-

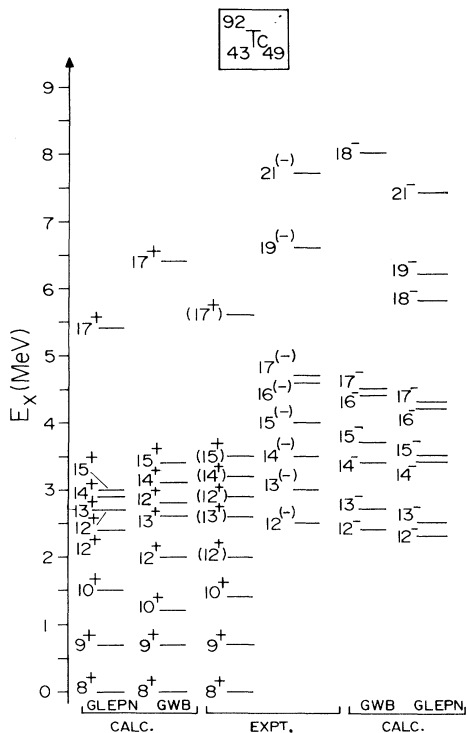


FIG. 9. Comparison of the experimental excitation energies in ^{92}Tc with shell model predictions. The notation GWB stands for the calculations using ^{66}Ni as the inert core. GLEPN notation indicates the calculations performed using ^{56}Ni as the closed core.

indicates that the many-body correlations are important and the coherence achieved by including a large number of configurations do indeed bring the level energies down. A point worth mentioning is that our calculations indicate that the $J = 16^+, 17^+, 18^-, 19^-$ and 21^- are dominated by the single neutron excitation across the $N = 50$ core.

V. CONCLUSIONS

The high-spin states in ^{92}Tc have been identified for the first time up to a tentative spin of $J = 17^+$ and 21^- . Nineteen new transitions have been identified and placed in the decay scheme.

Extensive shell model calculations involving enlarged configurations and different effective interactions were made to understand the observed level scheme of ^{92}Tc . The low-lying levels could be well understood within the $(p_{1/2}, g_{9/2})$ model space. For understanding the high-spin states in ^{92}Tc , shell model calculations were performed in an enlarged configuration space with ^{66}Ni as the core. This gave a reasonable agreement with the experimental data up to $J = 17$. The importance of many-body correlations is underlined by the result of these calculations—the energy required for the $N = 50$ neutron core breaking is brought down to about 2 MeV. Using a still larger model space with ^{56}Ni as the core, we were able to see further effects of these many-body correlations, resulting in a better agreement between the experimental level scheme and the shell model calculations.

ACKNOWLEDGMENTS

We gratefully acknowledge the helpful discussions with Professor A. P. Patro and Dr. S. K. Datta. We are thankful to Professor G. K. Mehta for his interest and encouragement. It is a pleasure to thank our colleagues S. Muralithar, G. O. Rodrigues, R. P. Singh, M. Gupta, and Dr. Pragya Singh for their help during the experiment analysis. Thanks are also due to the accelerator staff at the Nuclear Science Centre, New Delhi for their excellent cooperation. The authors S.S.G. and S.B.P. would like to acknowledge CSIR and BRNS respectively for the financial support for carrying out this research work.

- [1] S. S. Ghugre, S. B. Patel, M. Gupta, R. K. Bhowmik, and J. A. Shiekh, Phys. Rev. C **47**, 87 (1993).
- [2] S. S. Ghugre, S. B. Patel, M. Gupta, R. K. Bhowmik, and J. A. Shiekh, Phys. Rev. C **50**, 1346 (1994).
- [3] J. D. Ball, J. B. McGrory, and J. S. Larsen, Phys. Lett. **41B**, 581 (1972).
- [4] D. H. Gloeckner and F. J. D. Serduke, Nucl. Phys. **A220**, 477 (1974).
- [5] K. Muto, T. Shimano, and H. Horie, Phys. Lett. **135B**, 349 (1984).
- [6] M. Dasgupta, A. Navin, Y. K. Agarwal, C. V. K. Baba, H. C. Jain, M. L. Jhingan, and A. Roy, Pramana J. Phys. **38**, 291 (1992); Nucl. Phys. **A539**, 351 (1992).
- [7] C. A. Fields, F. W. N. DeBoer, and B. J. Diana, Nucl. Phys. **A401**, 117 (1983).
- [8] R. K. Bhowmik, S. Muralithar, G. O. Rodrigues, R. P. Singh, S. S. Ghugre and P. Mukherjee, Proceedings of DAE Symposium of Nuclear Physics (India) [Dept. of Atomic Energy Publication, Government of India, Vol. **35B**, p. 454 (1992)].
- [9] F. S. Stephens, M. A. Delenplanque, R. M. Diamond, A. O. Macchiavelli, and J. E. Draper, Phys. Rev. Lett. **54**, 2584 (1985).
- [10] T. Ishii, S. Garnsomsart, M. Ishii, Y. Saito, M. Nakajima, and M. Ogawa, JAERI **M 90-119**, 165 (1989).
- [11] F. J. D. Serduke, R. D. Lawson, and D. H. Gloeckner, Nucl. Phys. **A256**, 45 (1976).
- [12] R. Gross and A. Frenkel, Nucl. Phys. **A267**, 85 (1976).
- [13] B. A. Brown, A. Etchegoyen, W. D. Rae, and N. S. Godwin, OXBASH (unpublished).
- [14] F. J. D. Serduke, R. D. Lawson, and D. H. Gloeckner, Z. Phys. A **314**, 205 (1983).
- [15] J. Sinatkas, L. D. Skouras, D. Strottman, and J. D. Vergados, J. Phys. G **18**, 1401 (1992).
- [16] S. S. Ghugre and S. K. Datta, Proceedings of DAE Symp. of Nuclear Physics, India, 1993 (to be published).